# Exploring the conformational equilibrium of *E. coli* thioredoxin reductase: Characterization of two catalytically important states by ultrafast flavin fluorescence spectroscopy

PETRA A.W. VAN DEN BERG,[1] SCOTT B. MULROONEY,[2,5] BAS GOBETS,[3] IVO H.M. VAN STOKKUM,[3] ARIE VAN HOEK,[1] CHARLES H. WILLIAMS, JR.,[2] AND ANTONIE J.W.G. VISSER[1,4]

[1]MicroSpectroscopy Centre, Laboratory of Biochemistry, Wageningen University, Wageningen, The Netherlands
[2]Department of Veterans Affairs Medical Center, and Department of Biological Chemistry, University of Michigan, Ann Arbor, Michigan 48105, USA
[3]Faculty of Sciences, Division of Physics and Astronomy, Vrije Universiteit, Amsterdam, The Netherlands
[4]Department of Structural Biology, Institute of Molecular Biological Sciences, Vrije Universiteit, Amsterdam, The Netherlands

(RECEIVED February 15, 2001; FINAL REVISION July 10, 2001; ACCEPTED July 12, 2001)

**Abstract**

The conformational dynamics of wild-type *Escherichia coli* thioredoxin reductase (TrxR) and the mutant enzyme C138S were studied by ultrafast time-resolved fluorescence of the flavin cofactor in combination with circular dichroism (both in the flavin fingerprint and far-UV regions) and steady-state fluorescence and absorption spectroscopy. The spectroscopic data show two conformational states of the enzyme (named FO and FR), of which the physical characteristics differ considerably. Ultrafast fluorescence lifetime measurements make it possible to distinguish between the two different populations: Dominant picosecond lifetimes of ~1 ps (contribution 75%) and 7 ps (8%) are associated with the FO species in TrxR C138S. Long-lived fluorescence with two time constants in the range of 0.2–1 ns (total contribution 17%) originates from enzyme molecules in the FR conformation. The near absence of fast lifetime components in oxidized wild-type TrxR supports the idea of this enzyme being predominantly in the FR conformation. The emission spectrum of the FO conformation is blue-shifted with respect to that of the FR conformation. Because of the large difference in fluorescence characteristics, fluorescence measurements on time scales longer than 100 ps are fully determined by the fraction of enzyme molecules in the FR conformation. Binding of the thiol reagent phenyl mercuric acetate to wild-type enzyme and TrxR C138S stabilizes the enzymes in the FR conformation. Specific binding of the NADPH-analog, $AADP^+$, to the FR conformation resulted in dynamic fluorescence quenching in support of the multiple quenching sites model. Raising the temperature from 277K–323K resulted in a moderate shift to the FR conformation for TrxR C138S. High concentrations of the cosolvent glycerol triggered the domain rotation from the FO to the FR conformation.

**Keywords:** Flavin; conformation; protein dynamics; time-resolved fluorescence; thioredoxin reductase; fluorescence quenching

Reprint requests to: Dr. A.J.W.G. Visser, MicroSpectroscopy Centre, Laboratory of Biochemistry, Wageningen University, Dreijenlaan 3, 6703 HA Wageningen, The Netherlands; e-mail: Ton.Visser@laser.bc.wau.nl; fax: 31-317-484801.

[5]Present address: Department of Microbiology and Molecular Genetics, Michigan State University, East Lansing, Michigan, 48824-1101, USA

*Abbreviations:* $AAD^+$, 3-aminopyridine adenine dinucleotide; $AADP^+$, 3-aminopyridine adenine dinucleotide phosphate; CD, circular dichroism; DAS, decay-associated spectrum; DTNB, 5,5′-dithiobis(2-nitrobenzoic acid); DTT, 1,4-dithiothreitol; FAD, flavin adenine dinucleotide; FWHM, full width at half maximum; NADPH, reduced nicotinamide adenine dinucleotide phosphate; PMA, phenylmercuric acetate; TCSPC, time-correlated single photon counting; TrxR, thioredoxin reductase; wt TrxR, wild-type thioredoxin reductase; TrxR C138S, thioredoxin reductase with Cys138 mutated to Ser; TrxR C138S-PMA, thioredoxin reductase C138S treated with phenylmercuric acetate; TrxR wt-PMA, wild-type thioredoxin reductase reduced with NADPH and subsequently treated with phenylmercuric acetate and reoxidized.

Article and publication are at http://www.proteinscience.org/cgi/doi/10.1101/ps.06701.

Indications for the involvement of conformational dynamics in the catalytic mechanism of enzymes often arise from a conflict between structural and kinetic data. For many enzymes such as, for example, alcohol dehydrogenase (Eklund et al. 1981) and glutathione reductase (Pai and Schulz 1983), the resolution of the three-dimensional solution structure of the protein raised as many questions as it solved; prerequisites for catalysis such as substrate binding, product release, or interactions between different catalytic groups involved, could often not be clarified on the basis of the structural data. Mobility of the peptide chains then offers a likely explanation. For a number of enzymes, including examples like citrate synthase (Remington et al. 1982; Lesk and Chothia 1984) and adenylate kinase (Schulz et al. 1990; Gerstein et al. 1993), the occurrence of large conformational changes during catalysis has indeed been confirmed by X-ray structures of free protein and protein substrate (analog) complexes. Movements of complete protein domains can then play a prominent role (for review, see Gerstein et al. 1994).

From the point of view of domain motions, a particularly interesting enzyme is the flavoprotein, thioredoxin reductase, from *Escherichia coli*. Thioredoxin reductase (TrxR) is a member of the pyridine-nucleotide oxidoreductase family, which includes glutathione reductase, lipoamide dehydrogenase, and NADH peroxidase (for review, see Williams 1992, 1995). The enzyme catalyses the NADPH-dependent reduction of the single disulfide bridge in the protein substrate thioredoxin ($M_r$ = 11,700) (Moore et al. 1964; Holmgren 1968). Thioredoxin is involved in a variety of cellular processes, including ribonucleotide reduction (Thelander 1967; Holmgren 1989), and protein folding (Yasukawa et al. 1995).

The features and redox properties of TrxR enzymes from various organisms have been studied extensively (Williams 1992, 1995; Arscott et al. 1997, and references therein; Wang et al. 1999; Williams et al. 2000). The enzymes can be divided into two classes based on differences in molecular weight, amino acid sequence homology, and catalytic mechanism. High molecular weight thioredoxin reductases from higher eukaryotes resemble other oxidoreductases like glutathione reductase and lipoamide dehydrogenase in structure and mechanism (Arscott et al. 1997). However, low molecular weight TrxRs occurring in prokaryotes, fungi, and plants appear to be more distinctly related (Kuriyan et al. 1991; Arscott et al. 1997; Williams et al. 2000).

*E. coli* thioredoxin reductase (EC 1.6.4.5) is a homodimeric enzyme that contains one redox-active disulfide bridge and one molecule of FAD per subunit of $M_r$ = 35,300. The protein has a high affinity for the noncovalently bound flavin cofactor (Moore et al. 1964; Thelander 1967; Williams et al. 1967). *E. coli* thioredoxin reductase uses a ternary complex mechanism (Lennon and Williams 1995). During catalysis, the enzyme shuttles between the two-electron-reduced and four-electron-reduced state (Lennon and Williams 1996). From kinetic studies on the reductive half reaction of the enzyme, a three-phase mechanism has been proposed in which the rate-limiting step is attributed to a gross conformational change of the protein (Lennon and Williams 1997).

Indications for the requirement of a large conformational change first arose from the high-resolution crystal structure of the free enzyme (Kuriyan et al. 1991; Waksman et al. 1994). In these studies it was shown that each TrxR monomer consists of an NADPH-binding domain and an FAD-binding domain, connected by a double-stranded β-sheet. However, no obvious path for the flow of electrons from NADPH to the active-site disulfides via the flavin could be found. In the crystal structure, the active-site disulfides are buried in the protein interior near the flavin ring. However, there is no binding site present for thioredoxin, leaving dithiol–disulfide interchange with the protein substrate unexplained. Moreover, NADPH is bound 17 Å away from the flavin ring, with the nicotinamide ring positioned in a solvent-accessible area. Both NADPH and the disulfides are located on the *re*-side of the flavin in such a way that access of the NADPH to the isoalloxazine ring is blocked. By graphically rotating the NADPH domain over 66°, Waksman et al. (1994) showed that the problems of juxtaposition could be overcome. In the resulting model, the relative positioning of the FAD-binding and NADPH-binding domains is similar to that of other oxidoreductases such as glutathione reductase. Now, the nicotinamide C4 and the isoalloxazine N5 atoms are in close contact, with both rings parallel to each other, thus allowing efficient hydride transfer. In addition, the redox-active disulfides move to the surface of the protein where they become accessible for the protein substrate. Based on these findings, it was proposed that *E. coli* thioredoxin reductase has two conformational states: the form corresponding to the original crystal structure, in which the disulfide can oxidize the flavin (FO), and a conformation in which the rings of NADPH and FAD are juxtaposed, suitable for dithiol–disulfide interchange with thioredoxin and reduction of the flavin (FR) (Fig. 1).

To trap the enzyme in the FR conformation, crosslinked complexes have been constructed from mutant forms of thioredoxin and thioredoxin reductase that all had one of the two active-site cysteines mutated to serine. The remaining active-site cysteine in thioredoxin and TrxR was then used to form a covalent bond between the two proteins. Kinetic studies of TrxR C135S linked to thioredoxin C32S showed that this complex was locked in one conformation in which, indeed, FAD could be reduced by NADPH, but the electrons could not be transferred to the active-site disulfide (Wang et al. 1996). Similar results were reported for TrxR C138S complexed with thioredoxin C35S (Veine et al. 1998a).

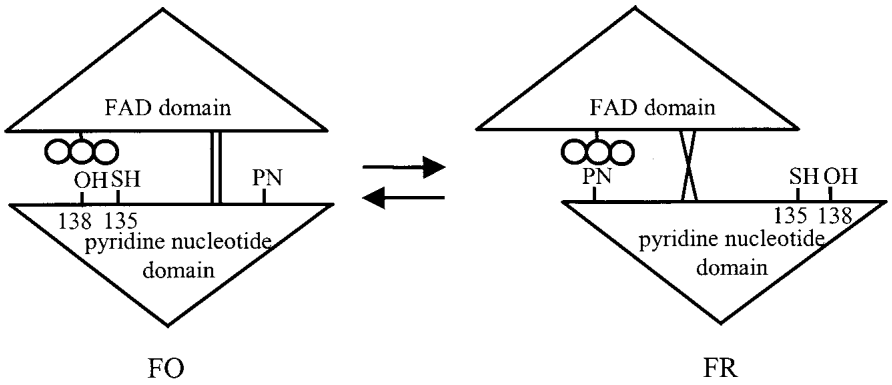


**Fig. 1.** Cartoon representation of TrxR C138S in the FO and FR conformations. The FAD and pyridine nucleotide domains are indicated as triangles and connected by lines depicting the double-stranded ß-sheet. The three circles represent the isoalloxazine ring of FAD, and PN indicates the pyridinium ring of the bound pyridine nucleotide. In the FR conformation, the flavin is in contact with the nicotinamide of bound NADPH or the aminopyridine of bound $AADP^+$; the remaining thiol is at the surface where it can react with thiol reagents stabilizing the FR conformation. In the FO conformation, Cys135 is buried close to the flavin and the pyridine nucleotide-binding site is exposed. Free enzyme in the FR conformation is relatively fluorescent, whereas in the FO conformation, fluorescence is quenched. Although the rotation between the FO and FR is shown as 180° in this illustration, it is actually 67°.

The properties of the mutant enzyme used in this study, TrxR C138S (Prongay et al. 1989), were recently reevaluated (Veine et al. 1998a). In contrast to wt TrxR, which has a flavin fluorescence quantum yield (Q) comparable to that of lipoamide dehydrogenase (Q = 0.1), TrxR C138S is only slightly fluorescent (7% of that of wt TrxR). This flavin fluorescence quenching was postulated as due to the proximity of Ser138 to the isoalloxazine ring, which occurs in the FO conformation (Mulrooney and Williams 1997). Steady-state flavin fluorescence studies on wt TrxR and TrxR C138S were performed to find support for the existence of FO and FR conformations in solution. It was proposed that in the mutant enzyme TrxR C138S, the FO conformation is stabilized by a hydrogen bond between the serine residue and the N5 atom of the flavin ring system. Results from intrinsic fluorescence spectra, fluorescence titrations with the thiol-specific reagent PMA and the NADPH analog $AADP^+$, as well as from absorption and limited proteolysis experiments, agreed with the model that in solution, the FO and FR conformations are in equilibrium. Only recently, crystal structure analyses of the crosslinked enzyme–protein substrate complex have indeed shown the existence of this FR conformation of *E. coli* thioredoxin reductase (Lennon et al. 2000): The structure of this complex resolved at 3.0 Å revealed a conformation in which the pyridine nucleotide domain was rotated by 67° with respect to the structure of the free enzyme.

More details of the conformational dynamics can be revealed using high time-resolution spectroscopic techniques. Time-resolved flavin fluorescence detection offers the unique possibility of probing the dynamic processes right on the site where catalysis occurs. The flavin fluorescence lifetime spectrum is very sensitive to the specific environment of the isoalloxazine and amino acid motions that alter this microenvironment. In addition, mobility of the flavin cofactor during the lifetime of the excited state can be visualized by time-resolved fluorescence anisotropy detection. Recent time-resolved flavin fluorescence studies on the oxidoreductases glutathione reductase and NADH peroxidase, have yielded profound information on the protein dynamics, conformational stability, and mechanism of fluorescence quenching in these enzymes (van den Berg et al. 1998; Visser et al. 1998).

In this study, time-resolved flavin fluorescence is used to monitor the conformational dynamics of *E. coli* thioredoxin reductase. Subpicosecond resolution fluorescence lifetime data in combination with fluorescence lifetime and fluorescence anisotropy data on a picosecond-to-nanosecond time scale, show two different protein conformational states and yield a picture of the dynamic behavior of the active site. Binding of substrate (analogs) and a specific thiol reagent is used to trap the enzyme in one conformational state. Variations in temperature and concentration of the cosolvent glycerol, serve as complementary approaches to influence conformational dynamics. Time-resolved fluorescence data are supported by fluorescence and absorption spectra and CD spectra in the visible light region, which show clear transitions in the direct microenvironment of the flavin.

## Results

### *Identification of the FO and FR conformation by ultrafast time-resolved fluorescence spectroscopy*

To explore the conformational dynamics of *E. coli* thioredoxin reductase, a series of four different protein/inhibitor combinations was investigated. This set consisted of wt

TrxR, TrxR C138S, and both proteins complexed to the specific thiol reagent PMA, yielding a phenylmercuric adduct on the (remaining) active-center cysteine residue. The choice of this combination was based on an earlier study (Mulrooney and Williams 1997), in which it was proposed that wt TrxR is mainly in the FR conformation, whereas in TrxR C138S, the equilibrium is shifted toward the FO conformation. PMA treatment would force the equilibrium to the FR conformer because of steric limitations of the phenylmercuric adduct. According to this model, the time-resolved fluorescence characteristics and the dynamic behavior of both PMA-treated proteins should be identical and should resemble those of wt TrxR, whereas TrxR C138S is expected to display different features.

Despite the large difference in fluorescence quantum yield of wt TrxR and TrxR C138S (14-fold), the flavin fluorescence intensity decays of all four proteins showed little difference when measured by subnanosecond-resolved time-correlated single-photon counting (Fig. 2A). Analysis of the fluorescence decay of wild-type protein at 293K yielded a fluorescence lifetime distribution containing two well-separated components of ~0.4 ns and 1.0 ns (Fig. 2B). These two lifetime components were found to be predominant in the lifetime spectra of TrxR C138S and the PMA-treated enzymes as well. The exact time constants of the components in the latter three enzymes were slightly shorter than in wt TrxR (difference of ~0.02–0.05 ns and 0.05–0.1 ns, respectively), whereas the relative amplitude of the longest lifetime was somewhat smaller (Table 1). These slight differences are indicative of a minor change in structure or dynamics of the microenvironment of the flavin. The lifetime spectra of both PMA-treated enzymes were identical. Besides the above-mentioned two predominant components, a short lifetime of ~100 ps was found to contribute to the fluorescence decay. The lifetime pattern of TrxR C138S contained an ultrafast component in most measurements. This component was analyzed to be on the order of 5 ps, which is on the border of the detection limit of the TCSPC setup used.

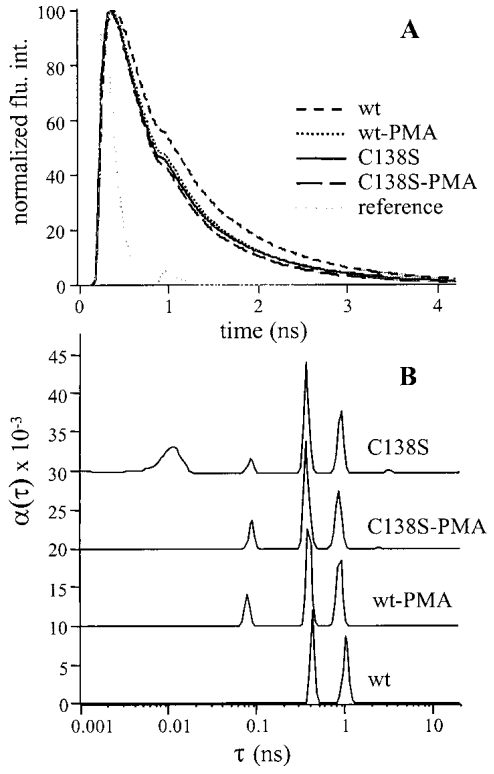


**Fig. 2.** The experimental total fluorescence decay (*A*) and fluorescence lifetime distributions (*B*) of wt TrxR, TrxR C138S, TrxR wt-PMA, and TrxR C138S-PMA in 50 mM potassium phosphate buffer (pH 7.6) at 293K. Experimental data (grey) and fitted data (black) overlie one another well and cannot be distinguished clearly. The experimental decay of the reference compound, erythrosine B ($\tau = 80$ ps), is also given. In the fluorescence lifetime spectra, a vertical offset has been applied for clarity. Because of the resolution limitations of the TCSPC setup used, the amplitude and time constant of the ultrafast component in TrxR C138S could not be determined accurately (see text).

The close resemblance of the fluorescence lifetime patterns of the four enzyme forms was difficult to reconcile with the clear differences found in absorption spectroscopy (Fig. 3A) and steady-state fluorescence intensity. CD spectra in the visible light region, the so-called flavin fingerprint spectra, confirmed the dissimilarity in the physical nature of the flavin microenvironment in TrxR C138S on the one hand, and those in wt TrxR and the PMA-treated enzymes on the other (Fig. 3B). Close inspection of the fitted fluorescence intensity decay of TrxR C138S revealed that the steep leading edge could not be fitted optimally with the lifetime component of ~5 ps. In addition, the amplitude of the ultrafast component as well as its precise time constant proved to be highly dependent on the exact analysis parameters. These features may suggest an extremely fast process on a subpicosecond time scale.

The possibility of such an ultrafast process was examined using subpicosecond- and wavelength-resolved fluorescence spectroscopy via a streak camera setup. With this method, the time resolution was increased up to 0.5–1 ps. The images, containing fluorescence intensity information in one dimension and spectral information in the second dimension, were analyzed through a global analysis procedure to yield the minimal number of spectral and temporal components needed to describe the data. Time traces of images of the proteins at 500 nm, showing both the experimental fluorescence intensity in the first 200 ps (partly logarithmic scale) and the corresponding fits, are presented in Figure 4. Now the enzymes show a clearly different picture: With TrxR C138S, the experimental time trace at 500 nm shows a predominant ultrafast decay, which is completely absent in that of wt TrxR.

For wt TrxR, analysis of the data again yielded two lifetime components, with time constants of 0.25 and 0.93 ns,

**Table 1.** *Temperature dependence of the barycenters and fractional contributions of the three longest fluorescence lifetime components of wt TrxR, TrxR C138S, and the PMA-complexes of both enzymes as measured with TCSPC*[a]

| | | 277K | 285K | 293K | 303K | 313K | 323K |
|---|---|---|---|---|---|---|---|
| wt | $\tau_1$ | – | – | – | 0.090 ± 0.02 | 0.090 ± 0.01 | 0.085 ± 0.01 |
| | $\alpha_1$ | – | – | – | 0.050 ± 0.01 | 0.12 ± 0.03 | 0.19 ± 0.04 |
| | $\tau_2$ | 0.55 ± 0.03 | 0.44 ± 0.01 | 0.42 ± 0.03 | 0.41 ± 0.02 | 0.39 ± 0.02 | 0.38 ± 0.01 |
| | $\alpha_2$ | 0.55 ± 0.05 | 0.52 ± 0.11 | 0.47 ± 0.06 | 0.49 ± 0.09 | 0.43 ± 0.09 | 0.41 ± 0.07 |
| | $\tau_3$ | 1.35 ± 0.05 | 1.15 ± 0.04 | 0.99 ± 0.05 | 0.93 ± 0.03 | 0.83 ± 0.02 | 0.79 ± 0.03 |
| | $\alpha_3$ | 0.44 ± 0.05 | 0.48 ± 0.11 | 0.51 ± 0.07 | 0.46 ± 0.09 | 0.44 ± 0.09 | 0.37 ± 0.06 |
| C138S | $\tau_{uf}$ | ++ | ++ | ++ | ++ | ++ | ++ |
| | $\alpha_{uf}$ | ++ | ++ | ++ | ++ | ++ | ++ |
| | $\tau_1$ | – | 0.11 ± 0.04 | 0.094 ± 0.02 | 0.089 ± 0.01 | 0.097 ± 0.01 | 0.092 ± 0.01 |
| | $\alpha_1$ | – | 0.06 ± 0.05 | 0.09 ± 0.02 | 0.12 ± 0.03 | 0.17 ± 0.03 | 0.22 ± 0.03 |
| | $\tau_2$ | 0.40 ± 0.01 | 0.39 ± 0.01 | 0.39 ± 0.01 | 0.36 ± 0.04 | 0.36 ± 0.01 | 0.35 ± 0.01 |
| | $\alpha_2$ | 0.62 ± 0.03 | 0.60 ± 0.09 | 0.56 ± 0.09 | 0.55 ± 0.09 | 0.54 ± 0.09 | 0.51 ± 0.06 |
| | $\tau_3$ | 1.04 ± 0.04 | 0.97 ± 0.03 | 0.92 ± 0.03 | 0.83 ± 0.03 | 0.78 ± 0.03 | 0.73 ± 0.02 |
| | $\alpha_3$ | 0.36 ± 0.02 | 0.35 ± 0.06 | 0.32 ± 0.05 | 0.30 ± 0.06 | 0.26 ± 0.05 | 0.27 ± 0.04 |
| wt-PMA | $\tau_1$ | – | 0.089 ± 0.01 | 0.093 ± 0.01 | 0.090 ± 0.01 | 0.089 ± 0.01 | 0.089 ± 0.01 |
| | $\alpha_1$ | – | 0.09 ± 0.02 | 0.14 ± 0.03 | 0.21 ± 0.04 | 0.24 ± 0.03 | 0.29 ± 0.02 |
| | $\tau_2$ | 0.42 ± 0.02 | 0.42 ± 0.02 | 0.40 ± 0.02 | 0.40 ± 0.02 | 0.38 ± 0.02 | 0.37 ± 0.01 |
| | $\alpha_2$ | 0.57 ± 0.11 | 0.50 ± 0.07 | 0.48 ± 0.09 | 0.47 ± 0.08 | 0.42 ± 0.06 | 0.44 ± 0.04 |
| | $\tau_3$ | 1.03 ± 0.04 | 0.97 ± 0.03 | 0.90 ± 0.03 | 0.84 ± 0.03 | 0.78 ± 0.02 | 0.78 ± 0.03 |
| | $\alpha_3$ | 0.44 ± 0.08 | 0.40 ± 0.06 | 0.39 ± 0.07 | 0.33 ± 0.06 | 0.30 ± 0.04 | 0.26 ± 0.02 |
| C138S-PMA | $\tau_1$ | – | 0.11 ± 0.02 | 0.11 ± 0.01 | 0.088 ± 0.01 | 0.086 ± 0.01 | 0.091 ± 0.01 |
| | $\alpha_1$ | – | 0.04 ± 0.02 | 0.13 ± 0.02 | 0.22 ± 0.02 | 0.29 ± 0.05 | 0.34 ± 0.04 |
| | $\tau_2$ | 0.41 ± 0.01 | 0.39 ± 0.01 | 0.39 ± 0.02 | 0.37 ± 0.01 | 0.36 ± 0.01 | 0.36 ± 0.01 |
| | $\alpha_2$ | 0.65 ± 0.12 | 0.60 ± 0.11 | 0.54 ± 0.06 | 0.48 ± 0.05 | 0.44 ± 0.07 | 0.43 ± 0.05 |
| | $\tau_3$ | 1.00 ± 0.03 | 0.91 ± 0.03 | 0.87 ± 0.04 | 0.82 ± 0.03 | 0.77 ± 0.02 | 0.76 ± 0.04 |
| | $\alpha_3$ | 0.35 ± 0.06 | 0.41 ± 0.07 | 0.31 ± 0.05 | 0.28 ± 0.04 | 0.26 ± 0.04 | 0.21 ± 0.04 |

[a] In TSCPC measurements, the time constant and amplitude of the ultrafast component could not be resolved accurately. The presence of this component in the lifetime spectra of TrxR C138S is therefore depicted with ++. Amplitudes were normalized excluding the amplitude of the ultrafast component. The lifetime spectra of wild-type TrxR revealed a component of 90 ps at temperatures of 303 K and higher, while the spectra of the TrxR C138S and the PMA-enzyme complexes revealed this component at temperatures from 285 K.

matching closely the TCSPC data. The DAS of these two lifetime components are identical and agree with the steady-state fluorescence spectrum of wt TrxR (Fig. 5A). For TrxR C138S, however, more lifetime components were needed to describe the fluorescence decay (Fig. 5B). Two ultrashort lifetimes of 1.2 and 7.3 ps determine the ultrafast fluorescence decay of the mutant enzyme with a main contribution of the 1.2 ps component (74.9% and 8.1%, respectively). The two long-lived components found correspond to those observed for wt TrxR, having identical decay associated spectra and again, as in the TCSPC experiments, somewhat shorter time constants (0.18 ns [contribution 5.5%] and 0.74 ns [11.6%], respectively). The DAS of the ultrashort components, however, are ~8 nm blue-shifted from those of the longer components and the spectra found for wild-type enzyme. In this case, it is legitimate to interpret the DAS as species-associated spectra: The ultrashort components are thus related to a separate conformational state in which the flavin experiences a completely different environment from that in wild-type enzyme. Based on the resolved amplitudes corresponding to the two enzyme species, 83% of the oxidized TrxR C138S is found in the FO conformation. As the dominant lifetime component is still close to the detection limit of the setup and any static fluorescence quenching occurring in the TrxR C138S enzyme is not taken into account, this percentage is expected to be an underestimation. (From a 14-fold difference in fluorescence quantum yield between wt TrxR and C138S, one would expect a population of FO conformers of ~90%, given the lifetime constants and ratios of amplitudes resolved in the streak camera experiments.)

The structure of the FO conformation can well explain the ultrarapid processes observed; in the crystal structure, the serine at 138 and the remaining active-site thiol at position 135, which both act as quenching sites, are at van der Waals distance of the flavin or closely to it (see Discussion). A charge-transfer reaction, such as a hydrogen or electron transfer from the thiol group, or a transient hydrogen bond between the hydroxyl group of the serine and the N5 atom of the flavin is likely to be the origin of the ultrafast processes observed. Wt TrxR in the FO conformation has the disulfide bridge juxtapositioned to the flavin instead of the above-mentioned quenching sites. Disulfide bridges, however, have also been reported as fluorescence quenching sites (van den Berg et al. 1998, and references therein). The absence of short fluorescence

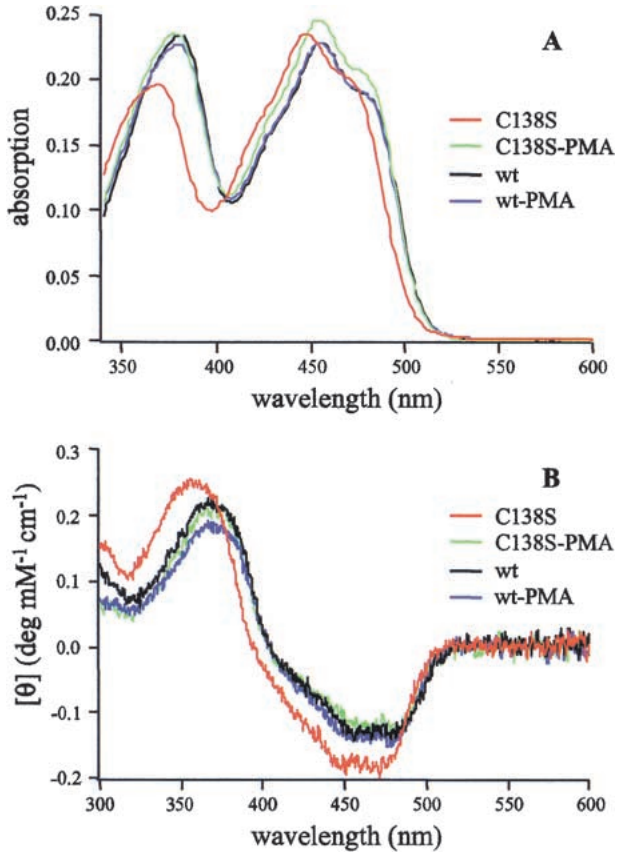


**Fig. 3.** Absorption spectra (*A*) and flavin fingerprint CD spectra (*B*) of 20 μM wt TrxR, TrxR C138S, TrxR wt-PMA ($\varepsilon_{456}$ estimated to be identical with wt TrxR), and TrxR C138S-PMA in 50 mM potassium phosphate buffer (pH 7.6) at 293K. The ellipticity is represented by θ.

lifetime components for wt TrxR is consistent with the idea that oxidized wild-type enzyme predominantly has the FR conformation (Mulrooney and Williams 1997). Although it could not clearly be resolved, a small population of FO conformers (estimated between 1% and 5%) might be hidden in the residual 16 ps lifetime component with an extremely low amplitude found in the fits of the wild-type enzyme (Fig. 5A). Experiments with the PMA-treated enzymes confirmed the interpretation of two conformational states: TrxR C138S-PMA and TrxR wt-PMA gave identical results with similar decay-associated spectra and lifetime components as found for wild-type enzyme, except for a minor contribution of a lifetime component near 0.05 ns. The ultrashort lifetime components found for TrxR C138S were completely absent in both PMA-treated enzymes. From the ultrafast fluorescence measurements, in combination with the other spectroscopic data presented, it can therefore be concluded that the PMA-treated enzymes are indeed fully restricted to the FR conformation.

*Substrate analog binding and the conformational state*

In the previous section it was shown that *E. coli* TrxR is locked in the FR conformation by reaction with the specific thiol-reagent PMA. Binding of substrates and substrate analogs may also shift the dynamic equilibrium and induce conformational transitions. A suitable analog for studying such an effect in TrxR is the oxidized NADPH analog, $AADP^+$, which binds to wt TrxR and the PMA-treated enzymes (Mulrooney and Williams 1997): In time-correlated single-photon counting experiments, binding of the analog resulted in an additional very short fluorescence lifetime component of ~10–15 ps (Fig. 6). The contribution of the longest lifetime diminished, whereas the contribution of the 100 ps component, which was observed in the PMA complexes but not previously in the free wt TrxR, was enlarged in all three enzymes. Even under saturating conditions (millimolar concentrations of $AADP^+$), all four fluorescence lifetime components remained present. These findings confirm the existence of multiple quenching sites that together determine the heterogeneous fluorescence decay originating from a single conformational state (the multiple quenching sites model): By binding $AADP^+$ to the FR conformers, an additional quenching site is introduced near the flavin, causing rapid fluorescence quenching. The phosphate moiety of

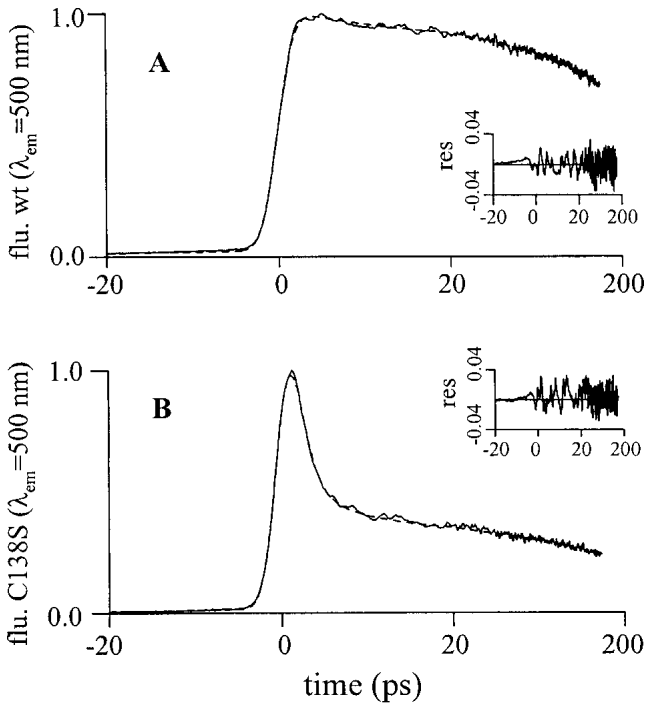


**Fig. 4.** Subpicosecond streak camera data of wt TrxR and TrxR C138S in 50 mM potassium phosphate buffer (pH 7.6) at 298K. Experimental time trace at 500 nm (solid) together with fit (dashed) of wt TrxR (*A*) and TrxR C138S (*B*). Insets show residuals. The time base from −20 to +20 ps (relative to the maximum of the instrument response) is linear, and from 20–200 ps is logarithmic.

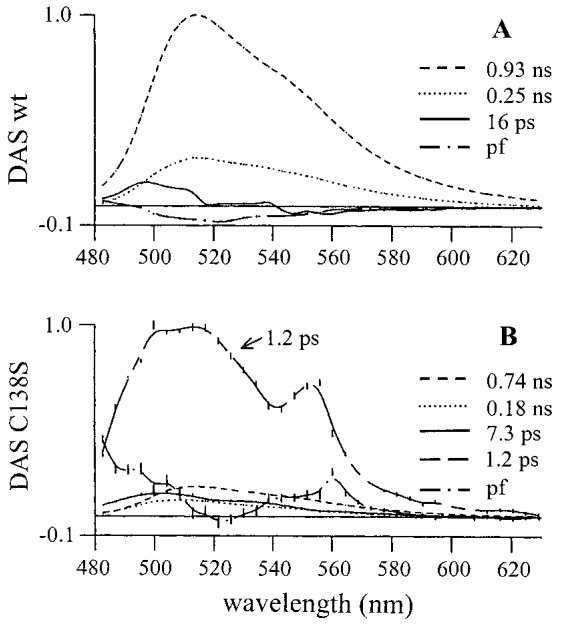


**Fig. 5.** Decay-associated spectra of the individual lifetime components of wt TrxR (*A*) and TrxR C138S (*B*). Vertical lines indicate plus or minus standard error in amplitude. Different DAS are depicted by different line types. Key *A*: 16 ps (solid), 0.25 ns (dotted), 0.93 ns (dashed), IRF follower (dot-dashed). Key *B*: 1.2 ps (chain-dashed), 7.3 ps (solid), 0.18 ns (dotted), 0.74 ns (dashed), IRF follower (dot-dashed). Raman scattering at ~555 nm is visible as a shoulder in the 1.2 ps DAS and as a peak in the IRF follower.

the $AADP^+$ appears to be essential for the binding of the NADPH analog. On titration with millimolar concentrations of the analog $AAD^+$, which lacks the phosphate moiety, no quenching of the flavin fluorescence was observed.

In contrast to wild-type enzyme, titration of the mutant enzyme TrxR C138S with $AADP^+$ did not lead to significant changes in the lifetime distribution. Because of the nature of free TrxR C138S, in which fluorescence is already strongly quenched, fluorescence quantum yields do not provide a sensitive tool to observe $AADP^+$-binding to this mutant enzyme. However, from the distinctive lifetime component introduced on $AADP^+$-binding, a conformational transition resulting from binding of this analog should have been easy to detect. This supports the earlier conclusion that $AADP^+$ cannot induce the conformational transition from FO to FR (Mulrooney and Williams 1997).

### *Probing the dynamic behavior*

The dynamic behavior of the TrxR enzymes was examined from fluorescence lifetime data as well as time-resolved anisotropy data. The temperature and viscosity dependencies of the lifetime spectra of the enzymes were determined in the range between 277K and 323K, using glycerol or sucrose as a cosolvent. Fluorescence anisotropy data were recorded to gain information on the mobility of the flavin cofactor. Given the extremely short fluorescence lifetime of the FO conformer, the anisotropy decay only provided information on the FR conformer. For all four enzymes, only fluorescence depolarization resulting from overall protein tumbling occurred, yielding a rotational correlation time of ~25 ns. The absence of any fast depolarizing processes shows that the flavin is rigidly bound; no mobility of the flavin cofactor occurs on the nanosecond time scale.

The effect of temperature on the fluorescence lifetime distributions was studied in the range between 277K and 323K by TCSPC and relative fluorescence quantum yield. The ability to detect changes in the dynamic equilibrium was thereby limited to an indirect approach, because the ultrafast component could not be well resolved. With increasing temperatures, all fluorescence lifetimes shifted to somewhat shorter time constants (Table 1). At low temperatures, the lifetime of ~100 ps did not appear in any of the lifetime spectra, whereas at high temperatures, it was visible in all spectra, including that of wt TrxR. This points more to a slight difference in dynamic behavior between wt TrxR and the other enzymes than to a static structural difference. By comparing the lifetime spectra with the one of free FAD at 323K, it could be concluded that at this high temperature still no traces of free FAD appeared. Wt TrxR and both PMA-treated enzymes, over the range from 277K–323K, showed a gradual decrease in relative fluorescence intensity of ~50%, which corresponds to the changes observed in the lifetime spectra. For TrxR C138S, the fluorescence intensity did not alter significantly in the range between 277K and 293K. From 293K–323K, however, the enzyme showed a gradual increase in fluorescence intensity of ~50%. This effect can only be explained by a change in the conformational equilibrium toward the FR conformer. Taking into

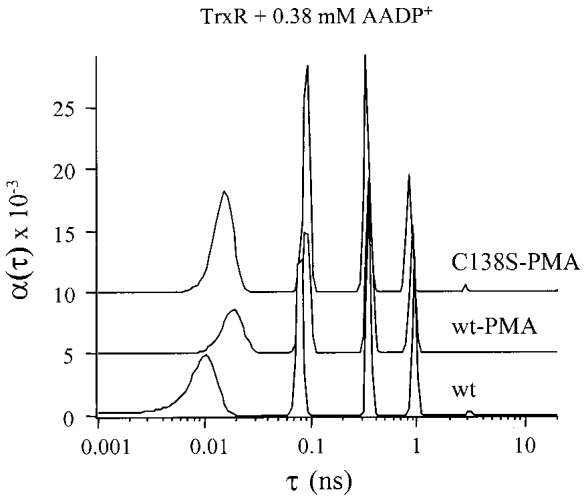


**Fig. 6.** Fluorescence lifetime distributions of wt TrxR, TrxR wt-PMA, and TrxR C138S-PMA complexed to 0.38 mM $AADP^+$ in 50 mM potassium phosphate buffer (pH 7.6) at 293K. For clarity a vertical offset has been applied.

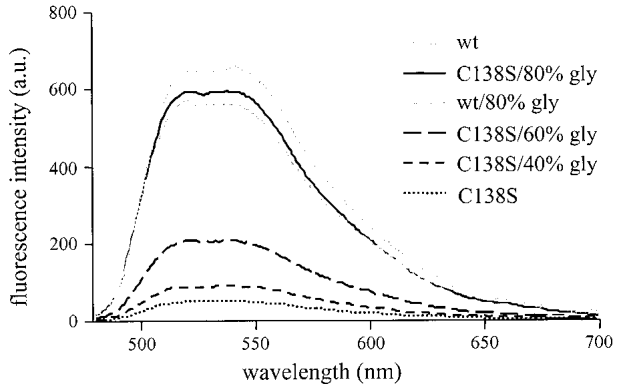


**Fig. 7.** Fluorescence spectra of 10 μM wt TrxR and TrxR C138S, as a function of percentage (v/v) glycerol, 50 mM potassium phosphate buffer (pH 7.6) at 293K. The spectra were corrected for the wavelength response of the setup.

account the decreasing fluorescence quantum yield of the other enzymes corresponding to the shift in lifetime constants, the increase in FR conformers can be estimated to be 100%–150% (from 277K–323K). Apparently the applied change in kinetic energy alone is not sufficient to induce major changes in the dynamic equilibrium.

A pronounced effect on the equilibrium was found using glycerol as a cosolvent: Whereas the quantum yield of wt TrxR in 80% v/v glycerol was ~10% lower than in buffer without glycerol, the fluorescence of the C138S enzyme increased to a level identical to that of wild-type enzyme in 80% glycerol (Fig. 7). The fluorescence lifetime patterns of the enzymes were only slightly influenced by the high concentrations of glycerol: For all enzymes, including TrxR C138S, the ratio of the amplitudes of the two longest lifetime components (~0.35 and 0.9 ns) gradually changed with increasing glycerol concentration from 1:1 to 3:2 in favor of the shorter time constant. In addition, for wt TrxR a shift of the longest component to a time constant identical to that of the other enzymes was found. The glycerol effect on the fluorescence lifetime patterns corresponds with the small gradual decrease in fluorescence quantum yield of wt TrxR and the PMA-treated enzymes, but is in clear contradiction with the major increase in fluorescence for TrxR C138S in a high concentration of glycerol: This indicates strongly that glycerol can trigger the conformational change from the FO to FR conformation. These findings were confirmed by light absorption spectra of C138S, which clearly changed from the characteristic FO spectrum (peaks at 380 and 456 nm) to the FR spectrum (peaks at 368 and 448 nm) in high concentrations of glycerol (Fig. 8A). At moderate levels of glycerol (up to 40%), no spectral changes occurred, and the fluorescence intensity was comparable to that in pure buffer. In absorption as well as in fluorescence, the behavior of the PMA-treated enzymes was comparable to wild-type enzyme in high concentrations of glycerol. When using sucrose as a cosolvent (up to 64% w/w, yielding a viscosity similar to the 80% glycerol mixtures), only a minor effect on the fluorescence intensity, and no effects on the absorption spectra and fluorescence lifetime patterns, were found.

CD experiments provided further support for the effect of glycerol on the conformational equilibrium: Flavin fingerprint CD spectra in the visible region from 300–600 nm show a clear transition for C138S, going from the FO spectrum in pure buffer to the FR spectrum in high glycerol concentrations (Fig. 8B). The slight effect of 80% glycerol on the photophysical properties of wt TrxR and the PMA-treated enzymes may reflect a minor structural adjustment in the microenvironment of the flavin, but might also be explained by the effect of the altered solvent composition on the photophysics of the flavin; in the FR conformation, the flavin is to a large extent directly exposed to the solvent. Far-UV CD spectra showed that glycerol does not affect the secondary structure content of the TrxR enzymes: All four enzyme combinations have a virtually identical far-UV CD spectrum with or without glycerol as a cosolvent (data not shown). Therefore, it can be concluded that glycerol indeed

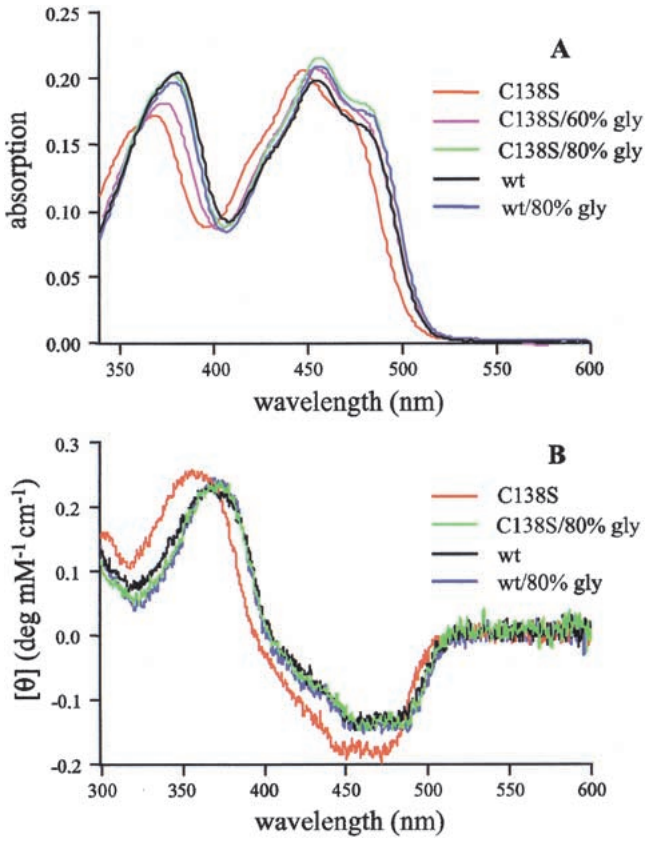


**Fig. 8.** Absorption spectra (*A*) and flavin fingerprint CD spectra (*B*) of 17.5 μM wt TrxR and TrxR C138S, as a function of percentage (v/v) glycerol, 50 mM potassium phosphate buffer (pH 7.6) at 293K. The ellipticity is represented by θ.

triggers the domain rotation, instead of just inducing a local conformational change.

## Discussion

*E. coli* TrxR is a beautiful example of nature's ingenuity in using protein dynamics to catalyze reactions with large substrates. The catalytic cycle, in which electrons flow from the substrate NADPH via the flavin cofactor and the disulfide bridge to the protein substrate thioredoxin, requires a major domain rotation. Earlier results from steady-state spectroscopic experiments and kinetic data on crosslinked protein substrate complexes strongly suggested the existence of two separate states with both involved in catalysis (Lennon and Williams 1995, 1996, 1997; Mulrooney and Williams 1997; Veine et al. 1998a,b; Wang et al. 1996). The crystal structure of the FR conformation recently resolved for the TrxR-thioredoxin crosslinked complex (Lennon et al. 2000) clearly shows the capacity of the protein to accommodate such large domain movements. Here we were able to show the presence of both states of the free enzyme in solution and to determine the specific photophysical characteristics of the FO and FR conformations. To directly detect the FO conformation and clearly distinguish between the two enzyme species, advanced fluorescence equipment was required that allows accurate analysis of states with fluorescence lifetimes in the (sub)picosecond range. The approach to use such ultrarapid photophysical processes to characterize the conformational dynamics of (flavo)proteins is quite new. Because of the limited time resolution of equipment regularly used in biochemical studies on protein fluorescence, such ultrarapid effects are either not resolved or ignored because of measurement inaccuracy. As a consequence, even in time-resolved fluorescence measurements, it is possible that not all existing conformational states that have different fluorescence characteristics, are observed. Obviously, as steady-state fluorescence measurements mainly detect conformations with a high fluorescence quantum yield, care has to be taken when interpreting these data. In this study, it is evident that because of the large difference in fluorescence quantum yield between the FO and FR conformation, measurements on time scales > 100 ps are fully determined by the fraction of enzyme molecules in the FR conformation (vide infra).

Recently, Mataga et al. (1998, 2000) have been the first to report on femtosecond fluorescence quenching in flavoproteins. By means of fluorescence upconversion, they were able to detect ultrarapid processes in the formerly so-called nonfluorescent flavoenzymes riboflavin-binding protein and glucose oxidase, and the D-amino acid oxidase benzoate complex. Although the study presented here is one of the first to report fluorescence quenching processes on the order of 1 ps, ultrarapid fluorescence quenching of protein-bound flavins seems a rather common event. For *E. coli* glutathione reductase and NADPH-peroxidase, we have shown earlier that a photoinduced electron transfer process from a juxtapositioned tyrosine residue to the flavin causes rapid fluorescence quenching, with lifetime components on the order of 5–15 ps (van den Berg et al. 1998; Visser et al. 1998). Strong indications exist that a similar mechanism applies to many other flavoproteins containing one or more tyrosine residues at Van der Waals distance of the flavin (van den Berg and Visser 2001). It should be emphasized that the observation of (ultrashort) fluorescence lifetimes originates from dynamic quenching as opposed to static quenching, which by definition originates from a ground-state complex. However, dynamic quenching should be interpreted in a broad sense; not only collisional quenching, but also interactions, such as electron or energy transfer that take place in the excited state, fall within this category. Therefore, the observation made in the previous study that fluorescence quenching in *E. coli* TrxR C138S has a static nature (Mulrooney and Williams 1997) is not completely correct, but results from a lack of time resolution in these experiments.

Based on the rapidity of the process, we expect that flavin fluorescence quenching in the FO conformer of TrxR C138S originates from a charge-transfer interaction with a residue located at Van der Waals distance from the flavin, resulting in a nearly instantaneous return to the ground state via a radiationless process. The only candidates for such a rapid charge-transfer interaction in TrxR C138S are Ser138 and the thiol group at position 135. These residues are only in close proximity of the electrophilic site of the flavin (N5 and C4a atoms) in the FO conformation (Table 2). In the FR conformation, these residues are shifted further away toward the side of the methyl groups of the flavin, which appears less favorable for fluorescence quenching (vide infra). Earlier, residue Ser138 had been proposed to be the predominant source of quenching (Mulrooney and Williams 1997): According to the crystal structure, this residue can form a hydrogen bond with the N5 atom of the flavin. Such a hydrogen bond will not only stabilize the FO conformation, but it will also provide a highly efficient pathway for photoinduced hydrogen transfer or electron transfer to this electrophilic site of the flavin. However, thiol groups are also known to be efficient fluorescence quenchers. An indication that both Ser138 and Cys135 are involved in the process of quenching may be derived from the presence of two ultrafast fluorescence lifetimes in the FO conformer. Based on the distance to the flavin, a logical assumption would be that Ser138 is responsible for the 1.2 ps lifetime and Cys135 for the 7 ps component. The rate constants corresponding to these fluorescence lifetimes (0.83 $ps^{-1}$ and 0.14 $ps^{-1}$) are in good agreement with the typical rate constants for electron transfer found for a variety of biological and (semi)synthetic systems with a donor–acceptor distance

**Table 2.** *Distances D between the isoalloxazine ring of* E. coli *TxrR and possible quenching sites located within 10 Å in the FO conformation and/or FR conformation. The expected efficiency of quenching Qef is expressed in H (high), M (moderate), and L (low).*

| | FO conformation[a] | | | FR conformation[b] | | |
|---|---|---|---|---|---|---|
| Res.-Atom | Flavin | D (Å) | Qef. | Flavin | D (Å) | Qef. |
| Ser/Cys138# | C4a | 2.5/3.1 | H | C7M | --/10.2 | L |
| (Ser-OH, Cys-SG) | N5 | 2.8/3.3 | H | | | |
| Cys/Ser135 | Ring B | 4.2–4.9/-- | H | C7M | --/6.7 | L[c] |
| Tyr118-OH | C7M | 3.5 | M/L | C8M | 11.4 | L |
| | N5 | 8.4 | M/L | N5 | 16.8 | L |
| Tyr023-OH | O2 | 3.6 | M[&] | O2 | 3.2 | M[d] |
| Trp52-CE3 | O2 | 5.7 | M | O2 | 5.8 | M |
| Cys303-SH | O2 | 7.0 | M | O2 | 6.9 | M |
| Phe142 | O4 | 6.2 | L | C7M | 16.4 | L |
| Phe240 | C7M | 8.5 | L | C7M | 10.3 | L |

Distances were retrieved from the crystal structures of:
[a] *E. coli* TrxR and (#) TrxR C138S resolved at 2 Å resolution (Waksman et al. 1994).
[b] *E. coli* TrxR C135S-Trx C35S crosslinked complex resolved at 3 Å resolution (Lennon et al. 2000).
[c] The hydroxyl/thiol group is directed away from the flavin ring.
[d] The tyrosyl group is located beside the flavin.

of 5 Å (1 $ps^{-1}$–0.1 $ps^{-1}$) (Moser et al. 1992, and references therein).

The idea that multiple fluorescence lifetimes can originate from various quenching processes that occur in a single protein conformation, the so-called multiple quenching sites model, was introduced by Bajzer and Prendergast (1993). By a theoretical description, they showed that the multiexponential fluorescence decay of several tryptophan-containing proteins can be explained by energy or electron transfer to different acceptor sites in the protein. These different processes, which in principle do not require any collisional interaction, all contribute to the deexcitation of the donor with a certain probability, thereby giving rise to more than one fluorescence lifetime. Studies on glutathione reductase and NADH peroxidase, in which by site-directed mutagenesis tyrosine and cysteine residues were replaced by aliphatic amino acid residues, have shown that this model is indeed valid; distinct fluorescence lifetimes could be attributed to quenching by a single amino acid residue (van den Berg et al. 1998; Visser et al. 1998). In the present study, clear evidence of the validity of the multiple quenching sites model is found in the lifetime patterns of wt TrxR and the PMA-treated enzymes saturated with $AADP^+$: Binding of this nicotinamide cofactor analog close to the flavin ring introduced an additional fluorescence lifetime component without further affecting the time constants of the protein (complexes) without $AADP^+$.

The presence of two long-lived fluorescence lifetimes for the FR conformation further supports this model. These lifetimes may result from interactions with quenching sites located further away or less well positioned for a charge-transfer interaction with the flavin. In general, electron-rich amino acid residues, such as tryptophans, tyrosines, and thiols, can be efficient quenching sites. Despite its aromatic character, phenylalanine appears to be a much less effective flavin fluorescence quencher (van den Berg et al. 1998). For intraprotein electron transfer, the rate of electron transfer has been shown to decay exponentially with the distance R between the donor and acceptor (Marcus and Sutin 1985, and references therein). In general, proper orbital overlap between the donor and acceptor favors charge transfer. For the orientation dependency of electron transfer, however, no specific laws are yet available. Based on these general relations and experimental evidence from various flavoenzymes, we can speculate on the efficiency of flavin fluorescence quenching in *E. coli* TrxR for possible quenching sites in the FO and FR conformations (Table 2): The orientation of quenching sites toward the methyl substituents and parallel to the xylene-like ring seems unfavorable. Highly efficient quenching rather seems to occur on interaction with the pi system of the polar pyrimidine- and pyrazine-like rings, especially near the electrophilic center of the molecule located at C4a and N5.

It should be stressed that the fluorescence lifetime distribution is only a representation of the ensemble average of distinctly different fluorescent conformations. In a dynamic equilibrium in which the enzyme shuttles between two (extreme) conformations, intermediate states can only be detected by (conventional) fluorescence methods, provided they have a significantly different fluorescence lifetime or correlation time distribution, and that the lifetime of the intermediate state (and related to this, the amplitude) is sufficiently large. These preconditions limit the chance of detecting intermediate states, especially when different sites contribute to fluorescence quenching in a single conformation. Because of the asymmetrical distribution of the strong quenching sites in the rotating domain (all close to the flavin in the FO conformation, none in the FR conformation), the situation for detecting intermediate states is here relatively favorable. The additional short lifetime emerging after PMA treatment might reflect the occurrence of such an intermediate state; it could, however, also originate from subtle structural changes in the microenvironment of the flavin.

Environmental factors, such as temperature and solvent composition, are known to have a pronounced effect on protein dynamics and may thus influence the conformational equilibrium. Whereas in this study the effect of temperature appeared to be limited, the importance of solvent composition is clearly shown by the effect of glycerol: High concentrations of glycerol clearly triggered the domain rotation from the FO to FR conformation. Besides its function as a viscogen, glycerol is also known to affect the hydration layer and volume of proteins (Timasheff et al. 1976; Gekko

and Timasheff 1981a,b; Timasheff 1993; Priev et al. 1996) and to induce structural changes (Raibekas and Massey 1996; van den Berg et al. 1998). The mechanism by which glycerol triggers the domain rotation in *E. coli* TrxR C138S should be sought in the effect on the interface between the FAD and NADPH domains; the hydration layer and in particular, the interactions that stabilize the FO conformation. Although in the FO conformation the flavin ring is more shielded from the solvent, the interface region is fairly solvent accessible (Waksman et al. 1994). It is possible that glycerol perturbs the interface region so that stabilizing interactions, such as the hydrogen bond between Ser138 and the flavin, can no longer be formed. The FAD and NADPH domains were found to have only two interdomain bonding interactions via hydrogen bonds, whereas five crystal water molecules mediated interdomain interactions between charged and polar residues on the interface (Waksman et al. 1994). In particular, the interdomain ion pair between Glu48 and Arg130, which protrudes into solution, forms an excellent target for glycerol. A recent study, in which these residues were mutagenized to cysteines to form a stable cross link with N,N,1,2 phenylenedimaleimide, indicated that this ion pair is indeed important for stabilization of the FO conformation (Veine et al. 1998b). The present study raises the question whether the cellular environment of the *E. coli* TrxR directly influences the catalytic control of the enzyme.

Although as yet the cellular mechanism that triggers domain rotation in *E. coli* thioredoxin reductase is still unknown, the approach of using ultrarapid fluorescence techniques has shed new light on the conformational equilibrium and protein dynamics of the enzyme. The study presented here proves the important additional value of subpicosecond time-resolved and spectrally resolved fluorescence for detecting and characterizing distinct protein conformations and for exploring the conformational space of flavoenzymes.

## Materials and methods

### *Enzymes and sample preparation*

Wt TrxR was purified from *E. coli* strain A326, which contains an insertion in the genomic TrxR gene (Russel and Model 1986), transformed with the recombinant plasmid pTrR310 (Mulrooney 1997). TrxR C138S was expressed from the recombinant plasmid pTrR336 as described elsewhere (Mulrooney and Williams 1997). Both enzymes were purified as described previously (Mulrooney 1997). Pure enzymes were stored in 80% ammonium sulfate at 277K. All chemicals used were of the highest purity available, and buffers were filtered through a 0.22 μm filter (Millipore).

After centrifugation, 1 mM of DTT was added to the resuspended TrxR C138S to remove potential sulfenic acid adducts on Cys135. For both wild-type and mutant TrxR, a Biogel PGD-6 column (Biorad) equilibrated with the appropriate measuring buffer, was used to remove undesired buffer contents and possible traces of free FAD. Standard spectroscopic measurements were performed in 50 mM potassium phosphate buffer (pH 7.6) at 293K. The enzyme concentration was based on the FAD content: $\varepsilon_{456}$ wt TrxR = 11.3 $mM^{-1}$ $cm^{-1}$ (Williams et al. 1967), $\varepsilon_{448}$ TrxR C138S = 11.8 $mM^{-1}$ $cm^{-1}$ (Mulrooney and Williams 1997). Preparation of TrxR C138S-PMA ($\varepsilon_{455}$ = 12.3 $mM^{-1}$ $cm^{-1}$) was performed by adding three to five equivalents of PMA to the protein after gel chromatography (Mulrooney and Williams 1997). For time-resolved fluorescence measurements, excess PMA was removed by gel filtration over a Biogel PGD-6 column. Wt TrxR was first anaerobically reduced by adding five equivalents of NADPH. After subsequent reaction with three equivalents of PMA for 15 min, the sample was reoxidized by air. Excess PMA and NADPH were removed from the enzyme preparations by a second gel filtration over a Biogel PGD-6 column. Samples containing glycerol were prepared by gently mixing the eluted protein with fluorescent-grade glycerol. As PMA-treatment did not induce changes in the absorbance spectrum of wt TrxR, the extinction coefficient of PMA-treated wild-type enzyme was assumed to be $\varepsilon_{456}$ TrxR wt-PMA = $\varepsilon_{456}$ wt TrxR = 11.3 $mM^{-1}$ $cm^{-1}$.

### *Steady-state spectroscopic measurements*

Absorption spectra were obtained using a Hewlett-Packard 8453 UV-Vis diode-array spectrophotometer with a resolution of 1 nm and an integration time of 0.5 sec. Steady-state fluorescence emission spectra were recorded on an SPEX Fluorolog 3-2.2 spectrofluorimeter with a slit width corresponding to a spectral resolution of 2 nm for both excitation and emission and an integration time of 1 sec. The spectra were corrected for the wavelength dependency of the setup. The samples had a maximum OD of 0.10 at the wavelength of excitation (450 or 456 nm). CD spectra were obtained using a Jasco 715 spectropolarimeter with a Jasco PTC 348 WI temperature controller. In the flavin fingerprint region (300–600 nm), four or nine spectra with a resolution of 0.2 nm, a scan speed of 50 nm/min and a response time of 1 sec were accumulated. In the far-UV region, typically nine or sixteen spectra (resolution 0.1 nm, response time 1 sec, scan speed 20 nm/sec) were averaged. Secondary structure determination was performed via ridge regression analysis with the CONTIN program based on a set of 16 protein structures (Provencher and Glöckner 1981). All steady-state spectroscopic measurements were performed at 293K and corrected for background contributions.

### *Time-resolved fluorescence and fluorescence anisotropy measurements*

Polarized time-resolved fluorescence experiments were performed using TCSPC. The complete TCSPC setup and the measurement procedures used were recently described in detail (van den Berg et al. 1998; Visser et al. 1998). A mode-locked CW Nd:YLF laser was used for synchronously pumping a cavity-dumped Stilbene 420 dye laser. The samples were excited with vertically polarized light of 450 nm with an excitation frequency of 594 kHz (duration 4 ps FWHM). Both parallel and perpendicular polarized fluorescence were detected through a 557.9 nm interference filter (Schott, Mainz, Germany, half bandwidth of 11.8 nm) in combination with a KV 520 cutoff filter (Schott). The data were collected in a multichannel analyzer with a time window of 1024 channels at a typical 7.0 ps/channel. The dynamic instrumental response function of the setup is approximately 40 ps FWHM, which makes registration of 5–10 ps lifetime components realistic. The instrumental response was obtained at the emission wavelength using erythrosine B in water ($\tau$ = 80 ps at 293K) as a reference com-

pound (Bastiaens et al. 1992). The temperature of the samples was controlled using a liquid nitrogen flow setup with a temperature controller (model ITC4, Oxford Instruments).

Analysis of the fluorescence intensity decay $I(t)$ and anisotropy decay $r(t)$ was performed using the software package from Maximum Entropy Solutions. With the maximum entropy method, the fluorescence intensity and anisotropy decays are described in terms of a continuous distribution of decay times, for which no a priori knowledge of the system is required. A detailed description of the principles of MEM and analysis of the polarized fluorescence data can be found elsewhere (Livesey and Brochon 1987; Bastiaens et al. 1992; Brochon 1994; van den Berg et al. 1998). The lifetime spectrum $\alpha(\tau)$ is obtained from the total fluorescence $I(t)$ via the inverse Laplace transform:

$$I(t) = E(t) * \int_0^\infty \alpha(\tau) e^{-t/\tau} d\tau \quad (1)$$

where $E(t)$ is the instrumental response function. The lifetime spectrum recovered consisted of 150 decay times equally spaced in log(t) space between 1 ps and 10 ns. The average fluorescence lifetime $<\tau>$ was calculated from the lifetime spectrum $\alpha(\tau)$, where N is the number of $\tau_i$ values of the $\alpha(\tau)$ spectrum:

$$\langle \tau \rangle = \frac{\sum_{i=1}^{N} \alpha_i \tau_i}{\sum_{i=1}^{N} \alpha_i} \quad (2)$$

### *Streak camera measurements*

The protein sample (30 μM) was mounted in a rotating optical cell with a light path of 3 mm. Measurements were performed at room temperature (298K). Femtosecond laser pulses were generated at a 100 kHz repetition rate using a titanium:sapphire-based oscillator (Coherent MIRA) and a regenerative amplifier (Coherent REGA), which pumped an optical parametric amplifier (Coherent OPA-9400), of which the 920 nm idler output was frequency doubled to create excitation light at 460 nm. The protein samples were excited with linearly polarized light with a wavelength of 460/462 nm, a pulse frequency of 200/125 kHz, and a pulse energy of ~5–10 nJ. The excitation light was put through a 15 cm focal length lens, resulting in a focus of 150 μm in the sample. The optical cell was rotated at 300 rpm to minimize protein damage by light accumulation effects. Flavin fluorescence was collected using a Hamamatsu C5680 synchroscan streak camera with a Chromex 250IS spectrograph with 8 nm resolution. Wild-type and C138S TrxR fluorescence was detected at a right angle to avoid contamination by scattered excitation light. The streak images were recorded on a Hamamatsu C4880 CCD camera, which was cooled to 218K. To optimize the accuracy of both short- and long-lived components, fluorescence data were recorded in two time windows of 200 ps and 2 ns, respectively. The FWHM of the time response of the system was 3–3.5 ps at the 200 ps time range and 15–20 ps at the 2 ns time range. The streak images were background subtracted and corrected for difference in sensitivity in the time domain by division by a streak image of a diffuse continuous white light source (shading correction). Wavelength-dependent temporal shifts of the time-zero point on the CCD image caused by the light collecting optics, the streak camera, and the spectrograph were corrected using white light pulses, for which the dispersion was calibrated using the optical Kerr signal in CS2 (Greene and Farrow 1983). The corrected and averaged images were reduced to a matrix of 950 points in time and 44 points in wavelength. Data of the 200 ps and 2 ns time windows were evaluated simultaneously in a global analysis fitting procedure (van Stokkum et al. 1993), in which the data were deconvolved with the (Gaussian-shaped) instrument response. The width of this Gaussian was a free parameter of the fit (typically, 3 ps FWHM). All measurements were analyzed using a model with parallelly decaying components, which yields DAS.

## Acknowledgments

We thank Willem van Berkel and Colja Laane for helpful discussions and suggestions. This work was supported by the Chemical Council of the Netherlands Organisation for Scientific Research (NWO).

The publication costs of this article were defrayed in part by payment of page charges. This article must therefore be hereby marked "advertisement" in accordance with 18 USC section 1734 solely to indicate this fact.

## References

Arscott, L.D., Gromer, S., Schirmer, R.H., Becker, K., and Williams, Jr., C.H. 1997. The mechanism of thioredoxin reductase from human placenta is similar to the mechanisms of lipoamide dehydrogenase and glutathione reductase and is distinct from the mechanism of thioredoxin reductase from *Escherichia coli*. *Proc. Natl. Acad. Sci.* **94:** 3621–3626.

Bajzer, Z. and Prendergast, F.G. 1993. A model for multiexponential tryptophan fluorescence intensity decay in proteins. *Biophys. J.* **65:** 2313–2323.

Bastiaens, P.I.H., van Hoek, A., Wolkers, W.F., Brochon, J.C., and Visser, A.J.W.G. 1992. Comparison of the dynamical structures of lipoamide dehydrogenase and glutathione reductase by time-resolved polarized flavin fluorescence. *Biochemistry* **31:** 7050–7060.

Brochon, J.C. 1994. Maximum entropy method of data analysis in time-resolved spectroscopy. *Methods Enzymol.* **240:** 262–311.

Eklund, H., Samama, J.P., Wallén L., Brändén, C.I., Åkeson, Å., and Jones, T.A. 1981. Structure of a triclinic ternary complex of horse liver alcohol dehydrogenase at 2.9 Å resolution. *J. Mol. Biol.* **146:** 561–587.

Gekko, K. and Timasheff, S.N. 1981a. Mechanism of protein stabilization by glycerol: Preferential hydration in glycerol-water mixtures. *Biochemistry* **20:** 4667–4676.

———. 1981b. Thermodynamic and kinetic examination of protein stabilization by glycerol. *Biochemistry* **20:** 4677–4686.

Gerstein, M., Schulz, G., and Chothia, C. 1993. Domain closure in adenylate kinase. Joints on either side of two helices close like neighboring fingers. *J. Mol. Biol.* **229:** 494–501.

Gerstein, M., Lesk, A.M., and Chothia, C. 1994. Structural mechanisms for domain movements in proteins. *Biochemistry* **33:** 6739–6749.

Greene, B.J. and Farrow, R.C. 1983. The subpicosecond Kerr effect in CS2. *Chem. Phys. Lett.* **98:** 273–275.

Holmgren, A. 1968. Thioredoxin. 6. The amino acid sequence of the protein from *Escherichia coli* B. *Eur. J. Biochem.* **6:** 475–484.

———. 1989. Minireview: Thioredoxin and glutaredoxin systems. *J. Biol. Chem.* **264:** 13963–13966.

Kuriyan, J., Krishna, T.S.R., Wong, L., Guenther, B., Pahler, A., Williams, Jr., C.H., and Model, P. 1991. Convergent evolution of similar function in two structurally divergent enzymes. *Nature* **352:** 172–174.

Lennon, B.W. and Williams, Jr., C.H. 1995. Effect of pyridine nucleotide on the oxidative half-reaction of *Escherichia coli* thioredoxin reductase. *Biochemistry* **34:** 3670–3677.

———. 1996. Enzyme-monitored turnover of *Escherichia coli* thioredoxin reductase: Insights for catalysis. *Biochemistry* **35:** 4704–4712.

———. 1997. Reductive half-reaction of thioredoxin reductase from *Escherichia coli*. *Biochemistry* **36:** 9464–9477.

Lennon, B.W., Williams, Jr., C.H., and Ludwig, M.L. 2000. Twists in catalysis: Alternating conformations of *Escherichia coli* thioredoxin reductase. *Science* **289:** 1190–1194.

Lesk, A.M. and Chothia, C. 1984. Mechanisms of domain closure in proteins. *J. Mol. Biol.* **174:** 175–191.

Livesey, A.K. and Brochon, J.C. 1987. Analyzing the distribution of decay constants in pulse-fluorimetry using the maximum entropy method. *Biophys. J.* **52:** 693–706.

Marcus, R.A. and Sutin, N. 1985. Electron transfers in chemistry and biology. *Biochim. Biophys. Acta* **811:** 265–322.

Mataga, N., Chrosrowjan, H., Shibata, Y., and Tanaka, F. 1998. Ultrafast fluorescence quenching dynamics of flavin chromophores in protein nanospace. *J. Phys. Chem. B* **102:** 7081–7084.

Mataga, N., Chrosrowjan, H., Shibata, Y., Tanaka, F., Nishina, Y., and Shiga, K. 2000. Dynamics and mechanisms of ultrafast fluorescence quenching reactions of flavin chromophores in protein nanospace. *J. Phys. Chem. B* **104:** 10667–10677.

Moore, E.C., Reichard, P., and Thelander, L. 1964. Enzymatic synthesis of deoxyribonucleotides. V. Purification and properties of thioredoxin reductase from *Escherichia coli* B. *J. Biol. Chem.* **239:** 3445–3452.

Moser, C.C., Keske, J.M., Warncke, K., Farid, R.S., and Dutton, P.L. 1992. Nature of biological electron transfer. *Nature* **355:** 796–802.

Mulrooney, S.B. 1997. Application of a single plasmid vector for mutagenesis and high level expression of thioredoxin reductase and its use to examine flavin cofactor incorporation. *Prot. Exp. Purif.* **9:** 372–378.

Mulrooney, S.B. and Williams, Jr., C.H. 1997. Evidence for two conformational states of thioredoxin reductase from *Escherichia coli*: Use of intrinsic and extrinsic quenchers of flavin fluorescence as probes to observe domain rotation. *Protein Sci.* **6:** 2188–2195.

Pai, E.F. and Schulz. G.E. 1983. The catalytic mechanism of glutathione reductase as derived from X-ray diffraction analyses of reaction intermediates. *J. Biol. Chem.* **258:** 1752–1757.

Priev, A., Almagor, A., Yedgar, S., and Gavish, B. 1996. Glycerol decreases the volume and compressibility of protein interior. *Biochemistry* **35:** 2061–2066.

Prongay, A.J., Engelke, D.R., and Williams, Jr., C.H. 1989. Characterization of two active site mutants of thioredoxin reductase from *Escherichia coli*. *J. Biol. Chem.* **264:** 2656–2664.

Provencher, S.W. and Glöckner, J. 1981. Estimation of globular protein secondary structure from circular dichroism. *Biochemistry* **20:** 33–37.

Raibekas, A.A. and Massey, V. 1996. Glycerol-induced development of catalytically active conformation of *Crotalus adamanteus* L-amino acid oxidase in vitro. *Proc. Natl. Acad. Sci.* **93:** 7546–7551.

Remington, S., Wiegand, G., and Huber, R. 1982. Crystallographic refinement and atomic models of two different forms of citrate synthase at 2.7 and 1.7 Å resolution. *J. Mol. Biol.* **158:** 111–152.

Russel, M. and Model, P. 1986. The role of thioredoxin in filamentous phage assembly. Construction, isolation and characterization of mutant thioredoxins. *J. Biol. Chem.* **61:** 14997–15005.

Schulz, G.E., Muller, C.W., and Diederichs, K. 1990. Induced-fit movements in adenylate kinases. *J. Mol. Biol.* **213:** 627–630.

Thelander, L. 1967. Thioredoxin reductase: Characterization of a homogeneous preparation from *Escherichia coli* B. *J. Biol. Chem.* **242:** 852–859.

Timasheff, S.N. 1993. The control of protein stability and association by weak interactions with water: How do solvents affect these processes? *Annu. Rev. Biophys. Biomol. Struct.* **22:** 67–97.

Timasheff, S.N., Lee, J.C., Pittz, E.P., and Tweedy, N. 1976. The interaction of tubulin and other proteins with structure-stabilizing solvents. *J. Colloid Interf. Sci.* **55:** 658–663.

van den Berg, P.A.W. and Visser, A.J.W.G. 2001. Tracking molecular dynamics of flavoproteins with time-resolved fluorescence spectroscopy. In *New Trends in Fluorescence Spectroscopy. Applications to Chemical and Life Sciences.* (eds. B. Valeur and J.C. Brochon), pp. 457–485. Springer, Berlin.

van den Berg, P.A.W., van Hoek, A., Walentas, C.D., Perham, R.N., and Visser, A.J.W.G. 1998. Flavin fluorescence dynamics and photoinduced electron transfer in *Escherichia coli* glutathione reductase. *Biophys. J.* **74:** 2046–2058.

van Stokkum, I.H.M., Brouwer, A.M., van Ramesdonk, H.J., and Scherer, T. 1993. Multiresponse parameter estimation and compartmental analysis of time resolved fluorescence spectra. *P. K. Ned. Akad. B Phys.* **96:** 43–68.

Veine, D.M., Mulrooney, S.B., Wang, P.F., and Williams, Jr., C.H. 1998a. Formation and properties of mixed disulfides between thioredoxin reductase from *Escherichia coli* and thioredoxin: Evidence that cysteine-138 functions to initiate dithiol-disulfide interchange and to accept the reducing equivalent from reduced flavin. *Protein Sci.* **7:** 1441–1450.

Veine, D.M., Ohnishi, K., and Williams, Jr., C.H. 1998b. Thioredoxin reductase from *Escherichia coli*: Evidence of restriction to a single conformation upon formation of a crosslink between engineered cysteines. *Protein Sci.* **7:** 369–375.

Visser, A.J.W.G., van den Berg, P.A.W., Visser, N.V., van Hoek, A., van den Burg, H.A., Parsonage, D., and Claiborne, A. 1998. Time-resolved fluorescence of flavin adenine dinucleotide in wild-type and mutant NADH peroxidase. Elucidation of quenching sites and discovery of a new fluorescence depolarization mechanism. *J. Phys. Chem. B* **102:** 10431–10439.

Waksman, G., Krishna, T.S.R., Williams, Jr., C.H., and Kuriyan, J. 1994. Crystal structure of *Escherichia coli* thioredoxin reductase refined at 2 Å resolution. Implications for a large conformational change during catalysis. *J. Mol. Biol.* **236:** 800–816.

Wang, P.F., Veine, D.M., Ahn, S.H., and Williams, Jr., C.H. 1996. A stable mixed disulfide between thioredoxin reductase and its substrate, thioredoxin: Preparation and characterization. *Biochemistry* **35:** 4812–4819.

Wang, P.F., Arscott, L.D., Gilberger, T.W., Müller, S., and Williams, Jr., C.H. 1999. Thioredoxin reductase from *Plasmodium falciparum*: Evidence for interaction between the C-terminal cysteine residues and the active site disulfide-dithiol. *Biochemistry* **38:** 3187–3196.

Williams, Jr., C.H. 1992. Lipoamide dehydrogenase, glutathione reductase, thioredoxin reductase, and mercuric ion reductase - A family of flavoenzyme transhydrogenases. In *Chemistry and Biochemistry of Flavoenzymes* (ed. F. Müller), Vol III, pp. 121–211. CRC Press, Boca Raton.

———. 1995. Mechanism and structure of thioredoxin reductase from *Escherichia coli*. *FASEB J.* **9:** 1267–1276.

Williams, Jr., C.H., Zanetti, G., Arscott, L.D., and McAllister, J.K. 1967. Lipoamide dehydrogenase, glutathione reductase, thioredoxin reductase, and thioredoxin. A simultaneous purification and characterization of the four proteins from *Escherichia coli* B. *J. Biol. Chem.* **242:** 5226–5231.

Williams, Jr., C.H., Arscott, L.D., Müller, S., Lennon, B.W., Ludwig, M.L., Wang, P-F., Veine, D.M., Becker, K., and Schirmer, R.H. 2000. Thioredoxin reductase – Two modes of catalysis have evolved. *Eur. J. Biochem.* **267:** 6110–6117.

Yasukawa, T., Kanei-Ishii, C., Maekawa, T., Fujimoto, J., Yamamoto, T., and Ishii, S. 1995. Increase of solubility of foreign proteins in *Escherichia coli* by coproduction of the bacterial thioredoxin. *J. Biol. Chem.* **270:** 25328–25331.